



# Sol–gel synthesis of Pd doped ZnO nanorods for room temperature hydrogen sensing applications

M. Kashif<sup>a,\*</sup>, M.E. Ali<sup>b</sup>, Syed M. Usman Ali<sup>c</sup>, U. Hashim<sup>a</sup>

<sup>a</sup>Nano Biochip Research Group, Institute of Nano Electronic Engineering (INEE), Universiti Malaysia Perlis (UniMAP), 01000 Kangar, Perlis, Malaysia

<sup>b</sup>Nanotechnology and Catalysis Research Centre, Universiti Malaya, 50603 Kuala Lumpur, Malaysia

<sup>c</sup>Department of Electronic Engineering, NED University of Engineering and Technology, Karachi 75270, Pakistan

Received 16 January 2013; received in revised form 24 January 2013; accepted 24 January 2013

## Abstract

A sol–gel spin coating technique was described for the synthesis of Pd doped ZnO nanorods for hydrogen sensing applications. The nanorods were hexagonal in shape, 50–100 nm in diameter and uniform in distribution. They exhibited homogeneous surface morphology, *c*-axis orientation and excellent crystalline properties. The synthesized nanorods were used to sense and detect hydrogen in a homemade gas chamber. The fabricated sensor successfully detected as low as 40 ppm hydrogen at room temperature with a very low level of power supply (16.16  $\mu$ A) under a mixed background. Dynamic and repeated responses were observed with a wide range of hydrogen concentrations (40–360 ppm) at 200 °C. The developed sensor was at least 25 fold more sensitive over the literature documented Pd doped ZnO nanorods in detecting hydrogen at ambient temperature. The simplicity, low-cost, high sensitivity and high stability of the sensor materials suggested that the synthesized Pd doped ZnO nanorods could be used in hydrogen and chemical sensing devices where Pd-mediated catalysis is involved.

© 2013 Elsevier Ltd and Techna Group S.r.l. All rights reserved.

**Keywords:** Pd doped ZnO nanorods; Hydrogen sensors; Sol–gel; Spin coating

## 1. Introduction

Over the recent years, Pd doped ZnO nanorods have received huge interest because of their applications in hydrogen sensors [1]. Hydrogen sensors are required for the detection of trace amount of hydrogen leaking from proton-exchange membrane and solid oxide fuel cells in spacecraft and other long-term devices [2]. These sensors must detect hydrogen at room temperature with minimal use of power and weight [3]. ZnO nanorods have large surface area, wide band gap and exciton energy [4]. They are also biocompatible, comparatively light in weight and considerably resistant to rust formation [5]. These properties have made ZnO nanorods and nanowires very

promising candidates for the determination of gas, humidity and chemical sensing devices [6,7].

Several studies have demonstrated that doped Pd on ZnO nanowires and nanorods enhances catalytic dissociation of molecular hydrogen into atomic hydrogen at room temperature [8]. Dissociation of molecular hydrogen into atomic hydrogen is a key step in the sensing and detecting mechanism of hydrogen. The predominant methods documented to synthesize ZnO nanorods for this particular application are chemical vapor deposition (CVD) and molecular beam epitaxy (MBE) [9]. However, both CVD and MBE methods involved high temperature growth and expensive instrumentations which are not available in ordinary laboratory settings. These techniques also need gold (Au) and/or other expensive metal coatings for the synthesis of ZnO nanorods and nanowires [8]. Moreover, Pd doping onto the synthesized ZnO requires RF sputtering which also needs expensive laboratory set-up [9].

Recently, the sol–gel spin coating technique has received enormous attention because of its simplicity, affordable

\*Corresponding author. Tel.: +60 49 798580, +60 49 798581; fax: +60 49 798578.

E-mail addresses: [kashif\\_bme@yahoo.com](mailto:kashif_bme@yahoo.com), [kashiff.farooq@gmail.com](mailto:kashiff.farooq@gmail.com) (M. Kashif).

instrumentations, low cost and controllable growth temperatures [10]. In this study, we synthesized *c*-axis aligned hexagonal ZnO nanorods with good crystalline and hydrogen sensing properties using a low-cost spin coating technique. Pd doping on the synthesized ZnO was performed using very simple instrumentations that require only micro-pipette and hot plate. To the best of our knowledge such a simple method is not described earlier in the published literature for the synthesis of Pd doped ZnO nanorods for the hydrogen detecting applications. Room temperature hydrogen sensing was investigated in a low cost home-made gas chamber. The simplicity and reproducibility of the method suggested its potential applications in large-scale synthesis of Pd doped ZnO nanorods for use in hydrogen, chemical and other gas sensing devices that involved Pd-mediated catalysis.

## 2. Experimental

ZnO nanorods were synthesized on silicon dioxide substrate as described in our previous research [10]. Briefly, zinc acetate dihydrate (98%, Sigma Aldrich) was mixed in 2-methoxyethanol (99.8%, Sigma Aldrich) where the molarity of Zn was maintained at 0.2 M. After 30 min stirring at room temperature, the hotplate temperature was ramped up to 60 °C. Monoethanolamine (MEA) (99%, Merck) was added drop-wise as a stabilizer under constant stirring. The molar ratio of MEA/Zn was maintained at 1:1. The stirring was continued until the solution turned into transparent from its initial whitish appearance. The prepared solution was aged for 24 h. An oxide layer of ~1 μm thickness was grown on a p-type silicon substrate of resistivity 1–50 Ω cm through a wet oxidation process. Prior to the oxide growth, the wafer was cleaned with RCA1 and RCA2 solutions followed by draining in dilute HF to remove the native oxide. An interdigitated electrode layer was deposited onto the oxide layer through Cr/Au evaporation using a hard mask and auto306 thermal evaporator. ZnO seed layer was deposited on the thermally oxidized silicon substrate using a spin coater rotating at 1000 rpm for 10 s and then ramped up to 3000 rpm for 45 s. After coating the seed layer, the film was dried at 250 °C for 20 min. The coating and drying processes were repeated 5 times. After depositing 5 successive layers, the sample was incubated in a furnace to anneal the thin film at 450 °C for 1 h under air atmosphere.

For the growth of ZnO nanorods, the prepared substrate was inserted inside a Teflon sample holder at the cut edges to keep the deposited side downward inside the growth solution. The growth solution was prepared by mixing zinc nitrate hexahydrate (99%, Sigma Aldrich) and hexamethyltetramine (99%), Merck) in DI water and the final concentration of the solution was maintained at 25 mM. The beaker was placed inside a preheated oven and the growth process was continued at 90 °C for 6 h. The prepared ZnO nanorods were washed in IPA and DI water to remove the excess and contaminated salts. Subsequently,

the synthesized ZnO nanorods were annealed at 450 °C for 1 h under air environment. For Pd doping, 0.01 M solution of Pd was prepared by mixing the required amount of palladium chloride (PdCl<sub>2</sub>, 99.999% Sigma Aldrich) in ethanol. The solution was stirred overnight to completely dissolve the Pd particles. Five microliter portion of the above solution was precisely transferred onto the synthesized ZnO nanorods using a micro-pipette and the whole mixture was heated at 250 °C for 5 min to dry out the residual chloride.

The structural properties of the Pd doped ZnO nanorods were investigated using an x-ray diffractometer (Bruker D8) with CuKα radiation at λ=1.5406 Å. The XRD pattern was recorded in the range of 20–60° operating at a voltage of 40 kV and a current of 40 mA. The material composition was analyzed using an x-ray photoelectron spectroscope (XPS) Omicron Dar400 (Omicron Germany). The chamber pressure was maintained at 2.4 e<sup>-10</sup> Torr throughout the measurement. Morphological studies were performed using a scanning electron microscope (JEOL JSM-6460LA). Gas sensing measurements were carried out in a homemade gas chamber of 3 L capacity. The base of the chamber was made up of stainless steel and the upper area was covered with a high vacuum glass dome. All the measurements were performed under atmospheric pressure. The chamber inlet was connected with an air pump and 1% H<sub>2</sub> in balance N<sub>2</sub> gas (Moxlinde, Malaysia). The flow of 1% H<sub>2</sub> gas was regulated using a mass flow controller (GFC-17, 0-100 ml/min, AALBORG, USA) whereas the air flow was controlled using a mass flow meter.

## 3. Results and discussion

The scanning electron micrograph of the synthesized Pd doped ZnO nanorods grown on thermally oxidized silicon substrate clearly demonstrated agglomerated Pd particles on few spots as well as at the corners of the ZnO nanorods (Fig. 1a). The diameter and length of the nanorods were 50–100 nm and 2–3 μm, respectively. The XRD spectra demonstrated two noticeable peaks at 34.5° (002) and 38.53° (211) planes (Fig. 1b). The sharp peak located at 34.5° (002) plane of the synthesized ZnO nanorods revealed their high quality crystals and *c*-axis orientation. The second peak at 38.53° (211) plane confirmed the presence of palladium oxide (PdO).

The study of the surface composition of the Pd doped ZnO nanorods using XPS spectroscopy reflected the presence of Zn, O, Pd and carbon (Fig. 2a). The carbon peaks were due to the unavoidable air exposure during insertion of the sample in an XPS chamber [11]. The peaks appearing at 284 eV and 288 eV were due to C–O and C=O bonds [12]. No other contaminants were detected on the Pd doped ZnO nanorod surfaces. The deconvoluted XPS spectra of ZnO and PdO regions of the nanorods are shown in Fig. 2 (b,c). The Pd doped ZnO nanorods produced two peaks at 1020 eV and 1043 eV that correspond to the distribution of Zn-2p<sub>3/2</sub> and 2p<sub>1/2</sub> core

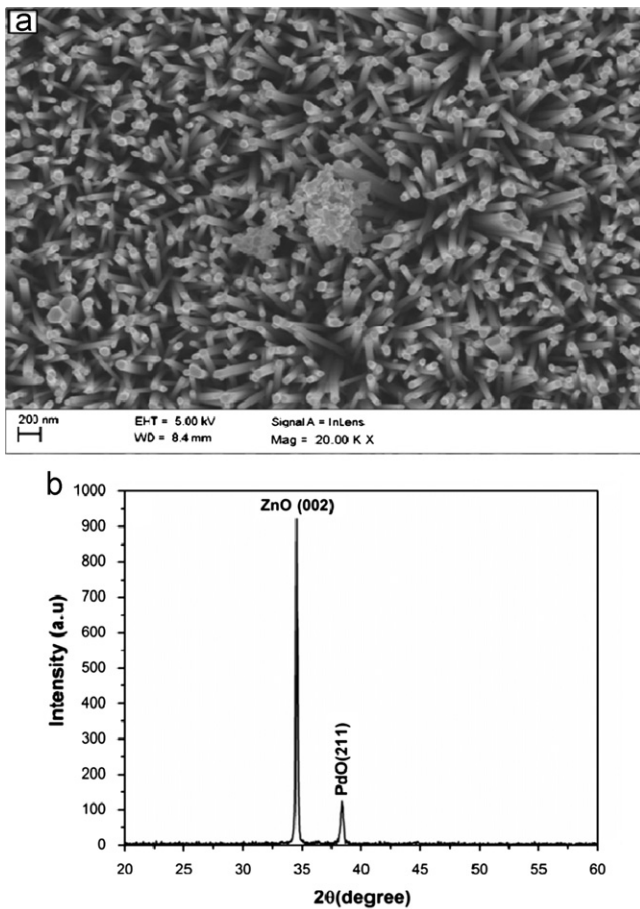


Fig. 1. (a) SEM image and (b) XRD pattern of Pd doped ZnO nanorods.

levels respectively [11]. The binding energy peaks for Pd  $3d_{3/2}$  and Pd  $3d_{5/2}$  core levels were observed at 340.82 eV and 334.7 eV respectively, reflecting the presence of doped Pd in the form of PdO in the ZnO nanorods.

The hydrogen detection ability of the Pd doped ZnO was tested in a homemade gas chamber under air and 1%  $H_2$  in balanced  $N_2$ . The characteristic  $I-V$  curves of Pd doped ZnO nanorods after exposure to various concentrations of hydrogen for 10 min at room temperature are represented in Fig. 3a. When the environment was switched from air to hydrogen, the sensor resistance was decreased and the current conduction was increased. For example, 47.5  $\mu A$  and 100.95  $\mu A$  of current flow was observed on exposure to 300 and 360 ppm of hydrogen gas, respectively. The sensor repeatedly detected 40 ppm hydrogen from room temperature to 200 °C temperatures without showing any saturation. The hydrogen sensitivity curve of Pd doped ZnO nanorods at room temperature is shown in Fig. 3b. The maximum sensitivity (1302%) was observed at 360 ppm of hydrogen. The sensitivity curve reflected that the fabricated device was 254% sensitive to 100 ppm hydrogen. This value was 25–63 folds higher over the literature documented reports [7–9]. Previous studies demonstrated only 4–10% sensitivity to 100 ppm hydrogen

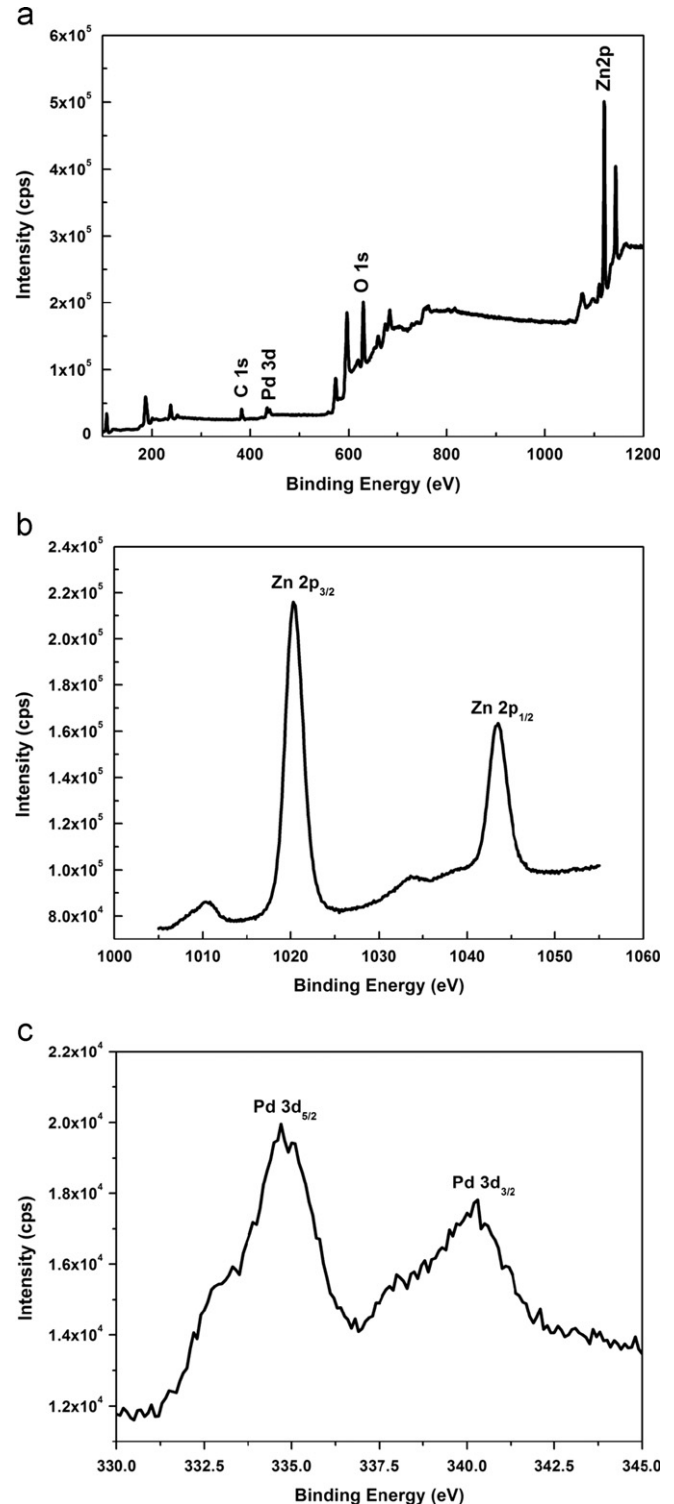


Fig. 2. XPS spectra of Pd doped ZnO nanorods: (a) survey spectra, (b) Zn 2p spectra and (c) the deconvolution spectra in Pd 3d region.

under similar experimental conditions for Pd doped ZnO nanorods. After each measurement, the sensor was heated up to 200 °C for the fast recovery of sensor from gas environment to air environment to obtain the original base value (Fig. 4). After that, the temperature was reduced to

room temperature and the sensor was ready for the next measurement cycle. The procedure was repeated for each measurement cycle.

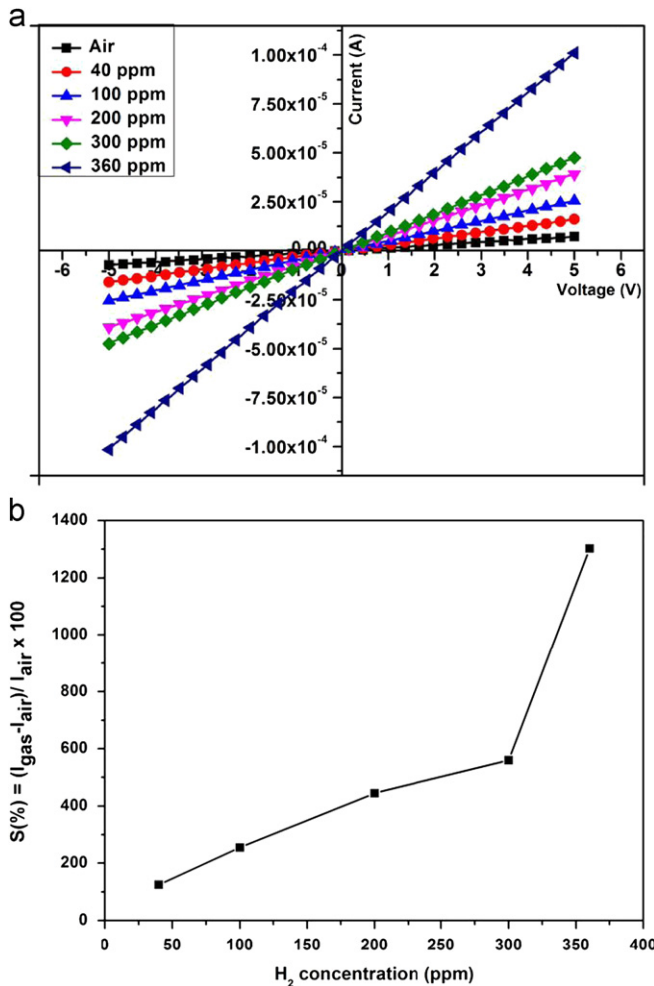


Fig. 3. (a)  $I$ - $V$  profile and (b) sensitivity curve for Pd doped ZnO nanorods as a function of hydrogen concentrations at room temperature.

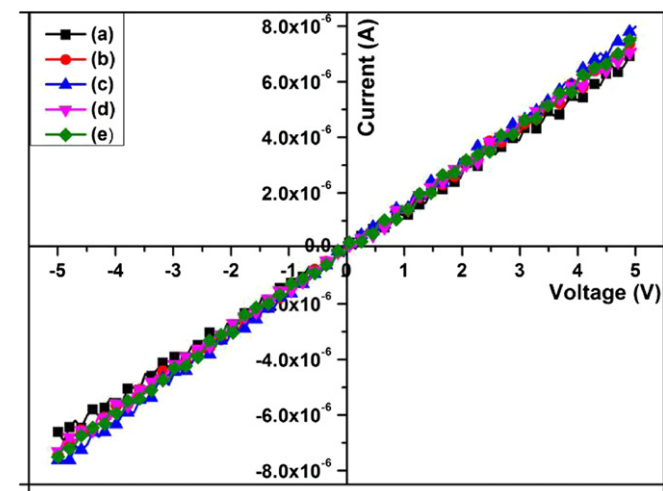


Fig. 4. Base line for the RT  $I$ - $V$  characteristics curve: (a) after 40 ppm, (b) after 100 ppm, (c) after 200 ppm, (d) after 300 ppm, and (e) after 360 ppm of hydrogen.

The dynamic responses of Pd doped ZnO nanorods were studied at 200 °C by exposing the sensor to variable concentration of hydrogen. The time versus current response and repeatability curves of the fabricated sensor are given in Fig. 5(a,b). The response and recovery time of the fabricated sensor were calculated at different hydrogen concentrations using the curve demonstrated in Fig. 5a. The response time was defined as the time taken by the sensor to achieve at least 90% variation in current flow with respect to its equilibrium value. The recovery time was the time taken by the sensor to achieve at least 10% variation in current flow to reach its initial value in air after the removal of hydrogen gas. The calculated values for the response and recovery time at 40, 100, 200, 300 and 360 ppm of hydrogen were found to be (41 s, 236 s), (55 s, 267 s), (69 s, 379 s), (71 s, 395 s) and (75 s, 441 s), respectively.

The sensor recovered and produced repeated signals after exposure to various hydrogen concentrations. Good reproducibility was observed even at high concentration (360 ppm hydrogen) and high operating temperature (200 °C). To

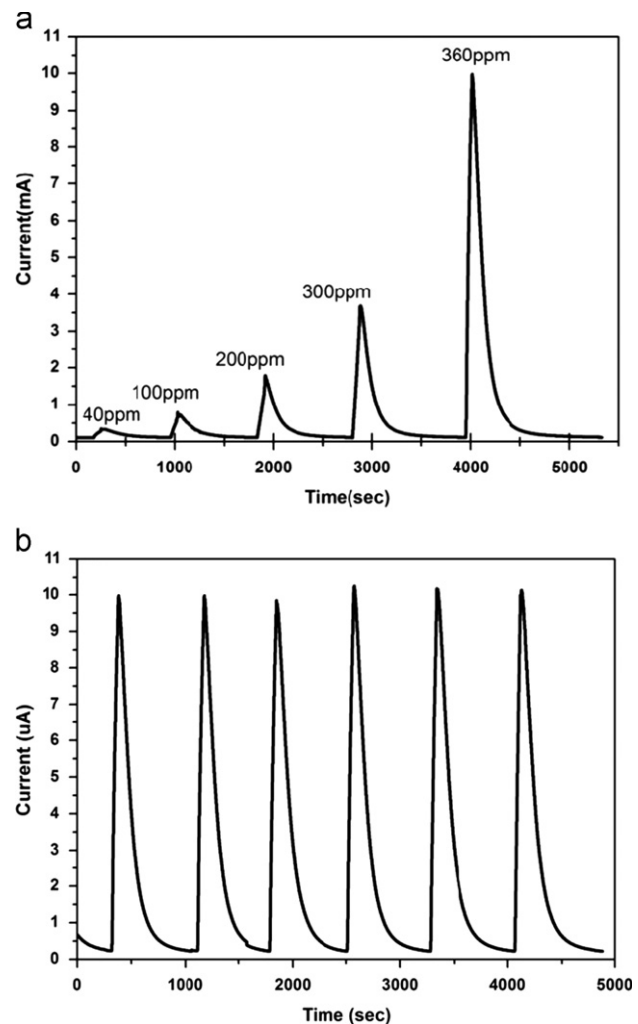


Fig. 5. (a) The dynamic response and (b) repeatability curves for Pd doped ZnO nanorods as a function of hydrogen concentrations at 200 °C.

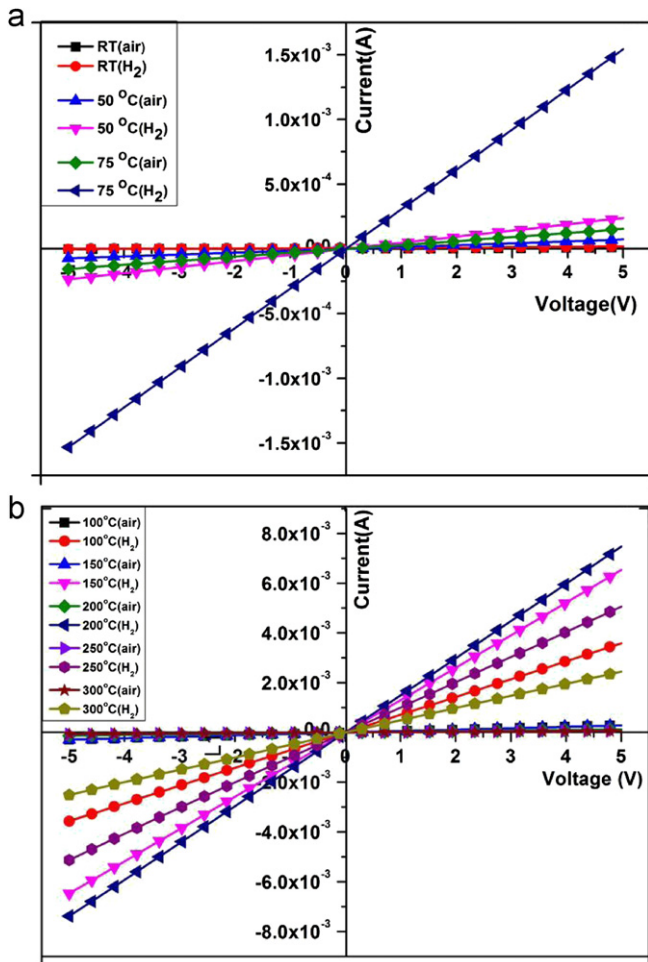


Fig. 6. *I-V* characteristics curve: (a) RT till 75 °C, (b) 100–300 °C with air and with 1% H<sub>2</sub> gas.

further investigate the temperature effect on the *I-V* curve, temperature was varied between 25 °C and 300 °C (Fig. 6). Repeated fall down of current flow was observed above 200 °C. This was because of the formation of chemisorption region where the oxygen molecules adsorbed onto the metal oxide surface that traps electron at elevated temperature (200–500 °C) [13].

The sensing phenomena of our proposed sensor were probably due to the reduction in electron concentration on the ZnO surface. ZnO initially adsorbs oxygen molecules from the ambient atmosphere. The adsorbed oxygen then extracts electrons from the conduction band of the ZnO and is converted into a single or a double oxygen ion and is ionisorbed on the ZnO surface [14]. This led to a decrease in electron concentration and consequently an increase in surface resistance. This mechanism can be described by the following equation [14,15]:



The reaction of hydrogen or any reduction gases with the ionisorbed  $O_{ads}^-$  results in the release of captured electrons back to the conduction band. This results in an increase in electron concentration, decreasing the resistance which

could be explained by the following reaction [14]:



The weak bonding of Pd atoms with the oxygen gas results in the dissociation of PdO at relatively low temperature releasing atomic oxygen. The created atoms migrate along the surface of the grains. This migration is induced by the catalyst atoms and is known as spill over of the gaseous ions [16,17]. Thus the oxygen atoms capture electrons from the surface layer forming an acceptor surface at the grain boundary. The presence of catalyst atoms activates the reaction between reducing gases and the adsorbed oxygen [18–21]. Thus the Pd sensitization on the ZnO nanorods surface enabled the hydrogen sensing at relatively low operating temperature.

#### 4. Conclusions

Pd doped ZnO nanorods were synthesized using a sol-gel spin coating technique for hydrogen sensing applications. The ZnO nanorods were of good crystalline properties and *c*-axis aligned with hexagonal morphology. The Pd sensitization was performed avoiding any expensive and complicated machinery. The synthesized Pd doped ZnO nanorods reproducibly detected ppm level hydrogen at room temperature with superior sensitivity and stability. All these advantageous features suggest its strong potential to be used in hydrogen sensing applications.

#### Acknowledgments

M. Kashif acknowledges financial support of the Malaysian Ministry of Higher Education (MOHE) through FRGS Grant no. 9003-00276 to Professor U. Hashim. The authors are thankful to the technical staff of Institute of Nano Electronic Engineering and School of Microelectronic Engineering in Universiti Malaysia Perlis for their kind support in performing this research.

#### References

- [1] O. Garcia-Serrano, O. Goiz, F. Chavez, G. Romero-Paredes, R. Pena-Sierra, Pd-decorated ZnO and WO<sub>3</sub> nanowires for sensing applications, *IEEE Sensors* (2011) 998–1001.
- [2] S. Srinivasan, *Fuel Cells from Fundamental to Applications*, Springer, New York, 2006.
- [3] S. Fardindoost, A. Irajizad, F. Rahimi, R. Ghasempour, Pd doped WO<sub>3</sub> films prepared by sol-gel process for hydrogen sensing, *International Journal of Hydrogen Energy* 35 (2) (2010) 854–860.
- [4] M. Kashif, S.M. Usman Ali, M.E. Ali, H.I. Abdulgafour, U. Hashim, M. Willander, Z. Hassan, Morphological, optical, and Raman characteristics of ZnO nanoflakes prepared via a sol-gel method, *Physica Status Solidi A* 209 (1) (2012) 143–147.
- [5] S.M. Usman Ali, N.H. Alvi, Z. Ibupoto, O. Nur, M. Willander, B. Danielsson, Selective potentiometric determination of uric acid with uricase immobilized on ZnO nanowires, *Sensors and Actuators B: Chemical* 152 (2) (2011) 241–247.
- [6] M.M. Arafat, B. Dinan, S.A. Akbar, A.S.M.A. Haseeb, Gas sensors based on one dimensional nanostructured metal-oxides: a review, *Sensors* 12 (6) (2012) 7207–7258.

- [7] H.T. Wang, B.S. Kang, F. Ren, L.C. Tien, P.W. Sadik, D.P. Norton, S.J. Pearton, J. Lin, Detection of hydrogen at room temperature with catalyst-coated multiple ZnO nanorods, *Applied Physics A* 81 (6) (2005) 1117–1119.
- [8] H.T. Wang, B.S. Kang, F. Ren, L.C. Tien, P.W. Sadik, D.P. Norton, S.J. Pearton, J. Lin, Hydrogen-selective sensing at room temperature with ZnO nanorods, *Applied Physics Letters* 86 (24) (2005) 243503.
- [9] S. Ren, G. Fan, S. Qu, Q. Wang, Enhanced  $H_2$  sensitivity at room temperature of ZnO nanowires functionalized by Pd nanoparticles, *Journal of Applied Physics* 110 (8) (2011) 084312–084316.
- [10] M. Kashif, U. Hashim, M.E. Ali, S.M.U. Ali, M. Rusop, Z.H. Ibupoto, M. Willander, Effect of different seed solutions on the morphology and electrooptical properties of ZnO nanorods, *Journal of Nanomaterials* 2012 (2012) 6.
- [11] O. Lupan, G.A. Emelchenko, V.V. Ursaki, G. Chai, A.N. Redkin, A.N. Gruzintsev, I.M. Tiginyanu, L. Chow, L.K. Ono, B. Roldan Cuenya, H. Heinrich, E.E. Yakimov, Synthesis and characterization of ZnO nanowires for nanosensor applications, *Materials Research Bulletin* 45 (8) (2010) 1026–1032.
- [12] G. Machado, D.N. Guerra, D. Leinen, J.R. Ramos-Barrado, R.E. Marotti, E.A. Dalchiele, Indium doped zinc oxide thin films obtained by electrodeposition, *Thin Solid Films* 490 (2) (2005) 124–131.
- [13] N. Barsan, U. Weimar, Conduction model of metal oxide gas sensors, *Journal of Electroceramics* 7 (3) (2001) 143–167.
- [14] N.H. Al-Hardan, M.J. Abdullah, A.A. Aziz, Sensing mechanism of hydrogen gas sensor based on RF-sputtered ZnO thin films, *International Journal of Hydrogen Energy* 35 (9) (2010) 4428–4434.
- [15] O. Lupan, G. Chai, L. Chow, Novel hydrogen gas sensor based on single ZnO nanorod, *Microelectronic Engineering* 85 (11) (2008) 2220–2225.
- [16] K.V. Gurav, P.R. Deshmukh, C.D. Lokhande, LPG sensing properties of Pd-sensitized vertically aligned ZnO nanorods, *Sensors and Actuators B: Chemical* 151 (2) (2011) 365–369.
- [17] P. Mitra, A.P. Chatterjee, H.S. Maiti, ZnO thin film sensor, *Materials Letters* 35 (1–2) (1998) 33–38.
- [18] N. Yamazoe, Y. Kurokawa, T. Seiyama, Effects of additives on semiconductor gas sensors, *Sensors and Actuators* 4 (0) (1983) 283–289.
- [19] N. Yamazoe, J. Fuchigami, M. Kishikawa, T. Seiyama, Interactions of tin oxide surface with  $O_2$ ,  $H_2O$  and  $H_2$ , *Surface Science* 86 (0) (1979) 335–344.
- [20] M. Egashira, Y. Shimizu, Y. Takao, S. Sako, Variations in  $I-V$  characteristics of oxide semiconductors induced by oxidizing gases, *Sensors and Actuators B: Chemical* 35 (1–3) (1996) 62–67.
- [21] Y. Shimizu, N. Kuwano, T. Hyodo, M. Egashira, High  $H_2$  sensing performance of anodically oxidized  $TiO_2$  film contacted with Pd, *Sensors and Actuators B: Chemical* 83 (1–3) (2002) 195–201.